Not-so-complex logarithms in the Heston model

Christian Kahl* Peter Jäckel†

First version: 1st June 2005
This version: 8th January 2006

Abstract

In Heston's stochastic volatility framework [Hes93], semi-analytical formulæ for plain vanilla option prices can be derived. Unfortunately, these formulæ require the evaluation of logarithms with complex arguments during the involved inverse Fourier integration step. This gives rise to an inherent numerical instability as a consequence of which most implementations of Heston's formulæ are not robust for moderate to long dated maturities or strong mean reversion. In this article, we propose a new approach to solve this problem which enables the use of Heston's analytics for practically all levels of parameters and even maturities of many decades.

1 Introduction

The Heston stochastic volatility model is given by the system of stochastic differential equations

$$\mathrm{d}S_t = \mu S_t \mathrm{d}t + \sqrt{V_t} S_t \mathrm{d}W_S(t), \tag{1}$$

$$\mathrm{d}V_t = \kappa(\theta - V_t)\mathrm{d}t + \omega\sqrt{V_t}\mathrm{d}W_V(t) \tag{2}$$

with correlated Brownian motions $\mathrm{d}W_S(t)\mathrm{d}W_V(t) = \rho \mathrm{d}t$. Heston [Hes93] found a semi-analytical solution for pricing European calls and puts using Fourier inversion techniques. The price for a European Call with strike K and time to maturity τ can be expressed very similar to the Black-Scholes one, namely

$$C(S, K, V_0, \tau) = P(\tau) \cdot \left[\frac{1}{2}(F - K) + \frac{1}{\pi} \int_0^\infty (F \cdot f_1 - K \cdot f_2)\, \mathrm{d}u \right] \tag{3}$$

where f_1 and f_2 are

$$f_1 := \mathrm{Re}\left(\frac{\mathrm{e}^{-iu\ln K}\varphi(u - i)}{iuF} \right) \quad \text{and} \quad f_2 := \mathrm{Re}\left(\frac{\mathrm{e}^{-iu\ln K}\varphi(u)}{iu} \right), \tag{4}$$

with $F = S\mathrm{e}^{\mu\tau}$, and $P(\tau)$ is the discount factor to the option expiry date. The function $\varphi(\cdot)$ is defined as the log-characteristic function of the underlying asset value S_τ at expiry:

$$\varphi(u) := \mathsf{E}\left[\mathrm{e}^{iu\ln S_\tau} \right]. \tag{5}$$

*Department of Mathematics, University of Wuppertal, Gaußstraße 20, Wuppertal, D-42119, Germany, and Quantitative Analytics Group, ABN AMRO, 250 Bishopsgate, London EC2M 4AA, UK

†Head of credit, hybrid, commodity, and inflation derivative analytics, ABN AMRO, 250 Bishopsgate, London EC2M 4AA, UK

Note that by virtue of definition (5) we have

$$\varphi(0) = 1 \qquad \text{and} \qquad \varphi(-i) = F\ . \tag{6}$$

Equation (3) for the price of a call option given the log-characteristic function of the underlying asset at expiry is generic and applies to any model, stochastic volatility or otherwise. It can be derived directly by the aid of the general result from functional analysis that the Fourier transform of the Heaviside function is given by a Dirac and a hyperbolic component:

$$\int \mathrm{e}^{-2\pi i u x} h(x)\,\mathrm{d}x \;=\; \frac{1}{2}\delta(u) + \frac{1}{2\pi i u}\ . \tag{7}$$

Specifically for the Heston model, we have

$$\varphi(u) = \mathrm{e}^{C(\tau,u)+D(\tau,u)V_0+iu\ln F}\ . \tag{8}$$

The coefficients C and D are solutions of a two-dimensional system of ordinary differential equation of Riccati-type. They are

$$C(\tau,u) \;=\; \frac{\kappa\theta}{\omega^2}\left(\left(\kappa - \rho\omega u i + d(u)\right)\tau - 2\ln\left(\frac{c(u)\mathrm{e}^{d(u)\tau}-1}{c(u)-1}\right)\right), \tag{9}$$

$$D(\tau,u) \;=\; \frac{\kappa - \rho\omega u i + d(u)}{\omega^2}\left(\frac{\mathrm{e}^{d(u)\tau}-1}{c(u)\mathrm{e}^{d(u)\tau}-1}\right) \tag{10}$$

with the auxiliary functions

$$c(u) = \frac{\kappa - \rho\omega u i + d(u)}{\kappa - \rho\omega u i - d(u)}, \qquad d(u) = \sqrt{(\rho\omega u i - \kappa)^2 + i u\omega^2 + \omega^2 u^2}. \tag{11}$$

What remains to be done for the valuation of plain vanilla options is the numerical computation of the integral in equation (3). This calculation is made somewhat complicated by the fact that the integrands f_j are typically of oscillatory nature. Still, the integration can be done in a reasonably simple fashion by the aid of Gauss-Lobatto quadrature [GG00]. The real problem, however, starts when the functions f_j are evaluated as part of the quadrature scheme since the calculation of the embedded complex logarithm on the right hand side of equation (9) is not as straightforward as it may look at first sight.

2 Two types of complex discontinuity

The first obvious problem with the inverse Fourier transformation (3) is the choice of branch of the multivalued complex logarithm embedded in C in equation (9). This is a generic problem with option pricing calculations based on the inverse Fourier transformation (3) of an expression derived from the log-characteristic function. One suggestion in the literature to remedy this is to carefully keep track of the branch [SZ99, Lee05] along a discretised path integral of $f_j(u)$ as u goes from 0 to ∞.

Let us recall that the logarithm of a complex variable $z = a + ib = r\mathrm{e}^{i(t+2\pi n)}$ can be written as $t \in [-\pi, \pi]$ and $n \in \mathbb{Z}$

$$\ln z = \ln|r| + i(t + 2\pi n). \tag{12}$$

If we restrict our choice to the principal branch, the functions f_j as defined in equation (4) incur discontinuities as is shown in figure 1 for f_1. Integrating this function with an adaptive quadrature scheme will not only result in the wrong number (because the area under the discontinuous curve shown in figure 1 is not the same as the area under the continuity-corrected curve), it will also take unnecessarily long due to the fact that the adaptive routine refines the number of sampling points excessively near the discontinuity.

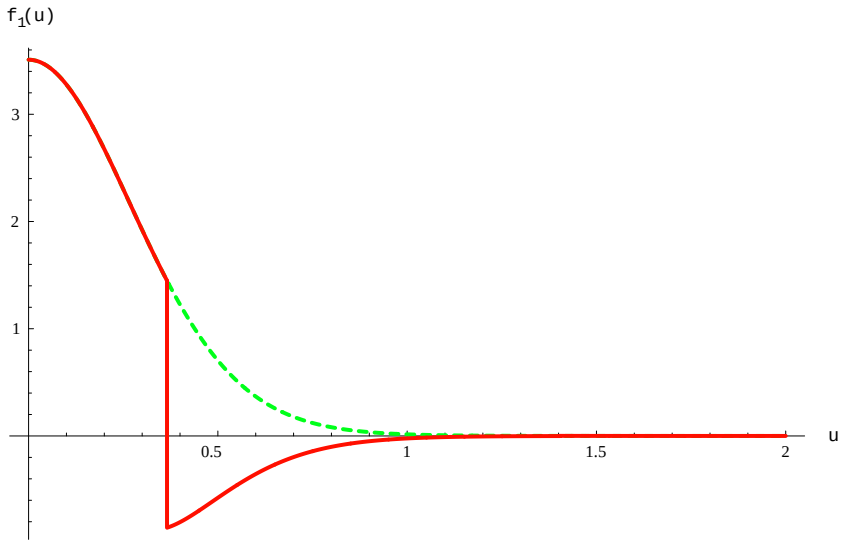

Figure 1: The function f_1 defined in (4). Underlying: $\mathrm{d}S_t = \mu S_t \mathrm{d}t + \sqrt{V_t} S_t \mathrm{d}W_S(t)$ with $S = 1$ and $\mu = 0$. Variance: $\mathrm{d}V_t = \kappa(\theta - V_t)\mathrm{d}t + \omega\sqrt{V_t}\mathrm{d}W_V(t)$ with $V_0 = 0.2$, $\kappa = 1$, $\theta = 0.2$, $\omega = 0.5$ and $\rho = 0.3$, time to maturity: $\tau = 30$, strike: $K = 1$, red curve: implementation using only the principal branche, green dashed curve: adjusted curve using formula (32)

In order to understand the mechanisms that gives rise to the discontinuity, we now examine more closely the component C defined in equation (9). To simplify the notation further on, we divide this term as follows:

$$C(\tau, u) = R(\tau, u) - 2\alpha \ln G(\tau, u) \tag{13}$$

$$R(\tau, u) := \alpha(\kappa - \rho\omega u i + d)\tau \tag{14}$$

$$\alpha := \frac{\kappa\theta}{\omega^2} \tag{15}$$

$$G(\tau, u) := \frac{c\mathrm{e}^{d\tau} - 1}{c - 1} \tag{16}$$

Looking at the whole function $\varphi(u)$ in (8), one could argue that it is not necessary to evaluate a complex logarithm at all since

$$\varphi(u) = G(\tau, u)^{-2\alpha} \mathrm{e}^{R(\tau,u) + D(\tau,u)V_0 + iu \ln F}. \tag{17}$$

This is true, though, we just shifted the problem from the logarithm to the evalutation of $G(u)^\alpha$ as this is exactly the part of the function where the jump arises. Indeed, if we try this formula in our implementation, the discontinuities do not go away (yet). The branch switching of the complex logarithm is in fact not the main problem that gives rise to the jumps of $f(u)$. A second effect is at work here and we will have to investigate further.

In the following, we make repeated use of the fact that, for any complex variable, we can choose either a real/imaginary part or a radius/phase[1] representation:

$$z = a_z + ib_z = r_z \mathrm{e}^{it_z}, \qquad t_z \in [-\pi, \pi)\ . \tag{18}$$

The fact that we restrict the phase $t_z \in [-\pi, \pi)$ means that we cut the complex plane along the negative real axis. Taking z to the power α gives

$$z^\alpha = r_z^\alpha \mathrm{e}^{i\alpha t_z}. \tag{19}$$

[1]Note that the phase, as we refer to it here, is also known as the *argument* and some mathematical software packages use the expression `arg` for the calculation of the phase of a complex number.

Whenever $G(u)$ crosses the negative real axis along its path (as u varies) the sign of the phase of $G(u)$ changes from $-\pi$ to π and therefore the phase of $G(u)^\alpha$ changes from $-\pi\alpha$ to $\pi\alpha$. This leads to a jump since

$$\mathrm{e}^{i\pi} = \mathrm{e}^{-i\pi} \Rightarrow \begin{cases} \mathrm{e}^{i\alpha\pi} \neq \mathrm{e}^{-i\alpha\pi} & \text{if } \alpha \notin \mathbb{Z} \\ \mathrm{e}^{i\alpha\pi} = \mathrm{e}^{-i\alpha\pi} & \text{else} \end{cases} \tag{20}$$

In other words, what appeared earlier as a problem with the branch choice of the multivalued complex logarithm in the evaluation of f given by equation (4) is in fact a problem with the ***branch switching of the complex power function*** which is related, though slightly different. To demonstrate this further, consider the case when, by coincidence, the parameter setting leads to $\alpha \in \mathbb{Z}$. In this scenario, there is no jump at all as we can see in figure 2. In general, though, we have $\alpha \notin \mathbb{Z}$. This wouldn't be a

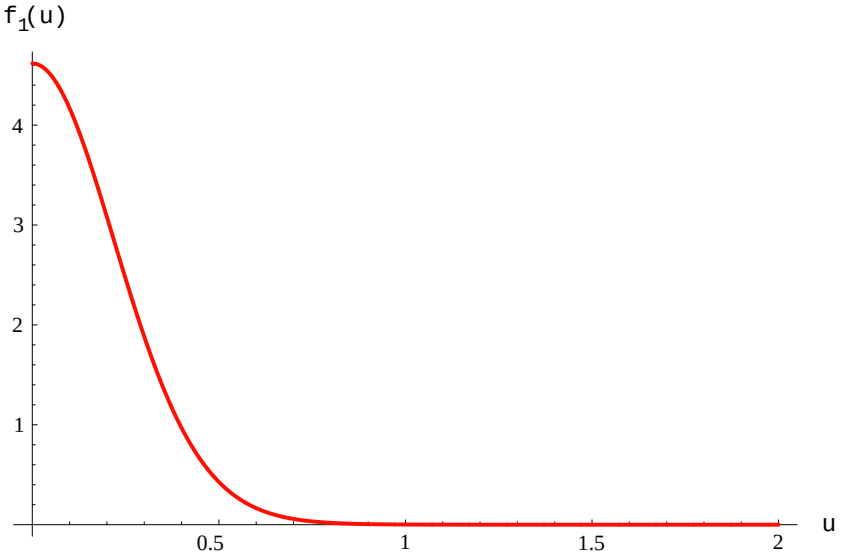

Figure 2: The function f_1 defined in (4) in the case that $\alpha \in \mathbb{Z}$. Underlying: $\mathrm{d}S_t = \mu S_t \mathrm{d}t + \sqrt{V_t} S_t \mathrm{d}W_S(t)$ with $S = 1$ and $\mu = 0$. Variance: $\mathrm{d}V_t = \kappa(\theta - V_t)\mathrm{d}t + \omega\sqrt{V_t}\mathrm{d}W_V(t)$ with $V_0 = 0.25$, $\kappa = 1$, $\theta = 0.25$, $\omega = 0.5$ and $\rho = 0.3$, exponent: $\alpha = -2$, time to maturity: $\tau = 30$, strike: $K = 1$.

problem if $G(u)$ didn't cross the negative real axis. However, as it turns out, the trajectory of $G(u)$ in the complex plane as u is varied from 0 to ∞, tends to start initially with a rapidly outwards moving spiral, prior to entering an asymptotic escaping behaviour. This is displayed in figure 3 for $G(u)$. Note that the shown trajectory is that of $\gamma(u) := G(u)\frac{\ln\ln|G(u)|}{|G(u)|}$, i.e. we have rescaled the coordinate system double-logarithmically in radius to compensate for the rapid outward movement of the spiralling trajectory of $G(u)$. The hue[2] $h \in [0, 1)$ of the curve is given by $h = \log_{10}(u + 1) \bmod 1$ which means that segments of slowly varying colour represent rapid movement of $G(u)$ as a function of u.

Another aspect why the correct treatment of the phase jumps of $G(u)$ is so important is the fact that it does not require unusual or particularly large parameters for the numerically induced discontinuity to occur. We show in figure 4 how the discontinuities in the complex phase of $G(u)$ arise simply as time to maturity is increased.

What we can learn from all of the above is that the only way to avoid the discontinuity of the integrands $f_j(u)$ altogether is to ensure that the phase of $G(u)$ is continuous. Various authors [SZ99, Lee05, Sep04] propose the idea to keep track of the number of jumps by comparing $G(u_k)$ and $G(u_{k+1})$ where u_k and u_{k+1} are adjacent points in their respective numerical integration scheme. This is an involved technical procedure leading to the need for a particularly complicated algorithm if we want to use an

[2] The *hue* is a number in the range $[0, 1)$ which varies the colour from red at 0 through the entire rainbow spectrum to purple (around 0.8), and then reconnecting to red at 1.

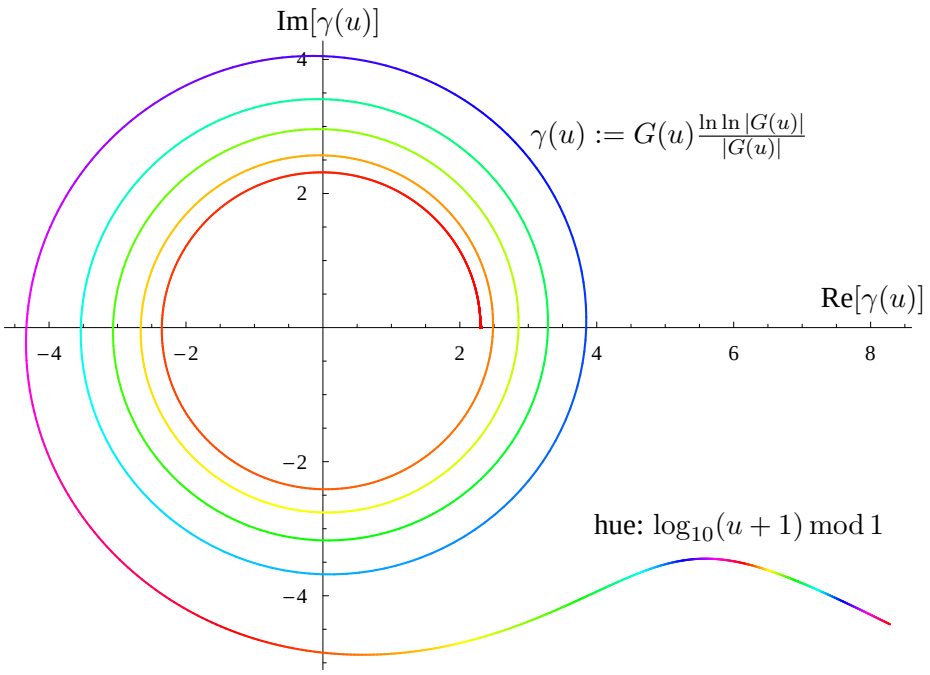

Figure 3: Part of the trajectory of the function $G(u)$ in the complex plane has the structural shape of a spiral which gives rise to repeated crossing of the negative real axis. Here: $\rho = -0.8$, $\kappa = 1$, $\omega = 2$, time to maturity $\tau = 10$.

adaptive quadrature method. Furthermore, we have to make sure that we account for *all* jumps which means that, for this to work reliably, we ought to have an estimate for the total number of discontinuities. Fortunately, however, there is a much simpler procedure to guarantee the continuity of $G(u)$ which we present in the following.

First, we introduce the notation

$$c =: r_c \mathrm{e}^{it_c}, \tag{21}$$

$$d =: a_d + ib_d. \tag{22}$$

The next step is to have a closer look at the denominator of G which was defined in equation (16):

$$\begin{aligned} c - 1 &= r_c \mathrm{e}^{it_c} - 1 \\ &=: r^* \mathrm{e}^{i(\chi^* + 2\pi m)} \end{aligned} \tag{23}$$

where

$$m := \mathrm{int}\left[\frac{t_c + \pi}{2\pi}\right] \tag{24}$$

$$\chi^* := \arg(c - 1) \tag{25}$$

$$r^* := |c - 1| \tag{26}$$

and with $\mathrm{int}[\cdot]$ denoting Gauss's integer brackets. Note that we have assumed $\arg(z) \in [-\pi, \pi) \, \forall \, z$. The key observation is that the subtraction of the number 1 from the complex variable c is simply a shift parallel to the real axis and therefore the phase of $(c - 1) \in [-\pi, \pi)$ if $t_c \in [-\pi, \pi)$, or in general, both χ^* and t_c can be assumed to be on the same phase interval. In other words, taking a complex number of arbitrary phase, and adding the real number -1, cannot possibly give rise to this operation moving the complex number across the negative real axis since this would require the addition of an imaginary component. This works as long as $c(u)$ never crosses the real axis in [0,1]. Fortunately, for $c(u)$, we have:

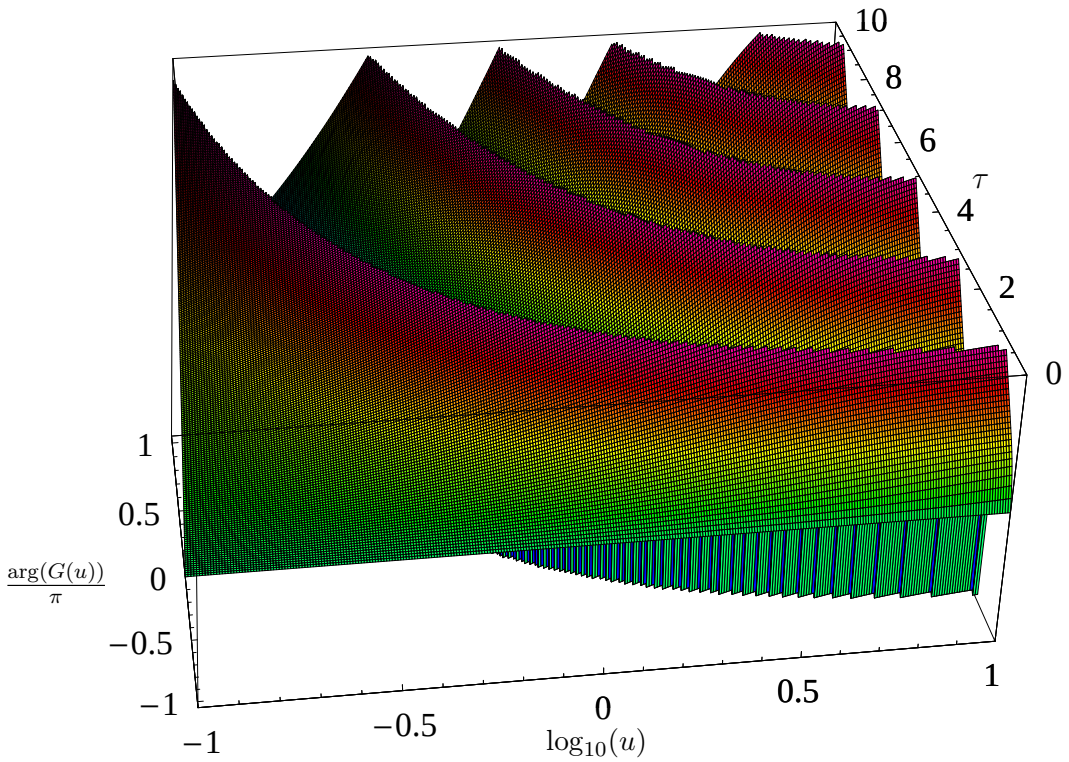

Figure 4: Without special handling, the phase of $G(u)$ incurs more and more jumps as time to maturity is increased. Here: $\rho = -0.8$, $\kappa = 1$, $\omega = 2$, time to maturity: $\tau \in [0, 10]$.

Proposition 2.1 The function $c(u)$ given in (11) only crosses the negative real axis.

The proof is given in the appendix.

We now do the same calculation with the numerator of G

$$ce^{d\tau} - 1 = r_c e^{it_c} e^{(a_d + ib_d)\tau} - 1 \tag{27}$$
$$= r_c e^{a_d \tau} e^{i(t_c + b_d \tau)} - 1$$

Defining

$$n := \text{int}\left[\frac{(t_c + b_d\tau + \pi)}{2\pi}\right] \tag{28}$$

$$\chi^{**} := \arg\left(ce^{d\tau} - 1\right) \tag{29}$$

$$r^{**} := \left|ce^{d\tau} - 1\right| , \tag{30}$$

we have

$$ce^{d\tau} - 1 = r^{**} e^{i(\chi^{**} + 2\pi n)}. \tag{31}$$

Again, we used the fact that the subtraction of 1 does not affect the rotation count of the phase of a complex variable as well as the fact that $c(u)e^{d(u)\tau}$ never crosses the real axis in [0,1]. The latter is guaranteed if the following holds:

Conjecture 2.2 The absolute value of the term $c(u)e^{d(u)\tau}$ is greater than 1.

Unfortunately, we have not been able to complete the proof of this conjecture as yet. However, extensive experiments have as yet not resulted in a single counterexample.

Combining these results we obtain

$$G(u) = \frac{c\mathrm{e}^{d\tau} - 1}{c - 1} = \frac{r^{**}}{r^{*}}\mathrm{e}^{i[\chi^{**} - \chi^{*} + 2\pi(n-m)]} \tag{32}$$

wherein the innocuous but crucial rotation count numbers m and n are given by equations (24) and (28). We are now in the position to compute the logarithm of $G(u)$ quite simply as

$$\ln G(u) = \ln(r^{**}/\, r^{*}) + i\,[\chi^{**} - \chi^{*} + 2\pi(n-m)]\,. \tag{33}$$

In figure 5, we show the rotation count corrected angle $\arg\left(G(u)\right)$ compared with the result by using just the principal branch of $G(u)$. We see that, without the correction, due to the sheer number of dis-

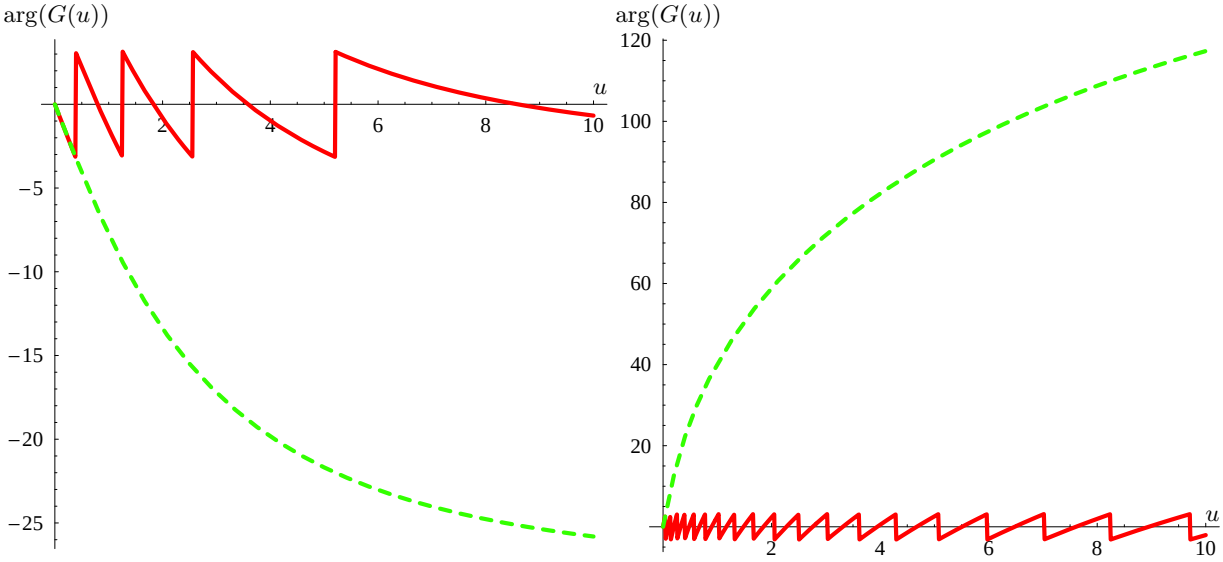

(a) (b)

Figure 5: The phase of $G(u)$ as defined in equation (16) with (dashed) and without (solid) rotation count correction given by equation (33), for $\kappa = 1$ and $\tau = 30$. (a) $\rho = 0.8$, $\omega = 0.5$. (b) $\rho = -0.95$, $\omega = 1.4$.

continuities, it can be very difficult indeed to keep track of the jumps by simply comparing neighbouring integration points. Note that it does not require the choice of unusual parameters: the discontinuities arise quite naturally for practically all choices of stochastic volatility configurations simply as time to maturity is increased, as was shown in figure 4.

The procedure for the discontinuity-corrected evaluation of function f_2 is summarized in algorithm 1. The evaluation of $f_1(u)$ is to be done by the same procedure with u replaced by $(u - i)$ in all but the last step of algorithm 1, with a subsequent division by the forward as one would expect from equation (4).

Remark 2.1 Whilst algorithm 1 is mathematically correct, it cannot actually be implemented directly in its presented form. For long times to maturity τ, the numerator term G_N can become very large which leads to numerical overflow. In order to avoid this, we can monitor the expression $\mathrm{Re}(d) \cdot \tau$: when this term becomes greater than $-\ln(\texttt{DBL\_EPSILON})$ we can neglect[3] the subtraction of 1 in steps 6 and 9 and the whole procedure of estimating the term $\ln(G(u))$ should be done in logarithmic coordinates.

3 Integration scheme

The choice of the right integration scheme is another crucial point for a robust implementation of the semi-analytical Heston solution. Due to the fact that the integrand can vary in its shape from almost

[3] The `C` header `<float.h>` provides the macro `DBL_EPSILON` which is defined as the smallest floating point number that, when added to the number 1, still results in a number that is distinct from 1 in the computer's floating point number representation.

Algorithm 1: Evaluate $f_2(u)$

Require: $F, K, \kappa, \theta, \omega, \tau > 0$,$V_0 \geq 0$ and $\rho \in (-1, 1)$

1: $\langle \mathbb{C} \rangle\ d := \sqrt{(\rho\omega ui - \kappa)^2 + \omega^2(ui + u^2)}$
2: $\langle \mathbb{C} \rangle\ c := \frac{\kappa - \rho\omega ui + d}{\kappa - \rho\omega ui - d}$
3: $\langle \mathbb{R} \rangle\ t_c := \arg(c)$
4: $\langle \mathbb{C} \rangle\ G_D := c - 1$ {Denominator of $G(u)$}
5: $\langle \mathbb{Z} \rangle\ m := \text{int}\left[\frac{t_c + \pi}{2\pi}\right]$
6: $\langle \mathbb{C} \rangle\ G_N := c\mathrm{e}^{d\tau} - 1$ {Numerator of $G(u)$}
7: $\langle \mathbb{Z} \rangle\ n := \text{int}\left[\frac{(t_c + \text{Im}(d)\tau + \pi)}{2\pi}\right]$
8: $\langle \mathbb{C} \rangle\ lnG := \ln(\text{abs}(G_N)/\,\text{abs}(G_D)) + i\,(\arg(G_N) - \arg(G_D) + 2\pi(n - m))$ {see (33)}
9: $\langle \mathbb{C} \rangle\ D := \frac{\kappa - \rho\omega ui + d}{\omega^2}\left(\frac{\mathrm{e}^{d\tau} - 1}{c\mathrm{e}^{d\tau} - 1}\right)$
10: $\langle \mathbb{C} \rangle\ C := \frac{\kappa\theta}{\omega^2}\left[(\kappa - \rho\omega ui + d)\tau - 2 \cdot lnG\right]$ {see (13)}
11: $\langle \mathbb{C} \rangle\ \varphi := \exp(C + D \cdot V_0 + iu\ln(F))$
12: $\langle \mathbb{R} \rangle\ f := \text{Re}\left[\frac{\exp(-iu\ln(K))\varphi}{iu}\right]$

simply exponentially decaying to highly oscillatory depending on the choice of parameters, most simple quadrature or numerical integration schemes are bound to fail significantly for some relevant scenarios. More advanced schemes such as the *adaptive Gauss-Lobatto* algorithm [GG00], however, are capable of handling the wide range of functional forms attainable by the integrand defined in (4). Since the Gauss-Lobatto algorithm is designed to operate on a closed interval $[a, b]$, we show below how one can transform the original integral boundaries $[0, \infty)$ to the finite interval $[0, 1]$, taking into account our knowledge of the analytical structure of the integrand for large u. Adapting the transformation to the asymptotic structure for $u \to \infty$ not only aids the stability of the adaptive quadrature scheme, it also makes the integration scheme significantly more efficient in the sense that far fewer evaluation points are needed.

Proposition 3.1 Assuming that $\kappa, \theta, \omega, \tau > 0$ and $\rho \in (-1, 1)$ we obtain the following asymptotics:

$$\lim_{u\to\infty} \frac{d(u)}{u} = \omega\sqrt{1-\rho^2} =: d_\infty \tag{34}$$

$$\lim_{u\to\infty} c(u) = -1 + 2\rho^2 + 2i\rho\sqrt{1-\rho^2} = \left(i\sqrt{1-\rho^2} + \rho\right)^2 \tag{35}$$

$$\lim_{u\to\infty} \frac{D(u)}{u} = -\frac{\sqrt{1-\rho^2} + i\rho}{\omega} \tag{36}$$

$$\lim_{u\to\infty} \frac{C(u)}{u} = -i\alpha\omega\rho\tau - \alpha d_\infty \tau \tag{37}$$

This leads to

$$\lim_{u\to\infty} f_j(u) \approx f_j(0) \cdot \mathrm{e}^{-uC_\infty} \cdot \text{Re}\left(\frac{\mathrm{e}^{iut_\infty}}{iu}\right) = f_j(0) \cdot \mathrm{e}^{-uC_\infty} \cdot \frac{\sin(ut_\infty)}{u} \tag{38}$$

with

$$C_\infty = \left(\alpha d_\infty \tau + \frac{\sqrt{1-\rho^2}}{\omega} V_0\right) = \frac{\sqrt{1-\rho^2}}{\omega}\left(V_0 + \kappa\theta\tau\right) \tag{39}$$

as well as

$$t_\infty = -\alpha\omega\rho\tau - \frac{\rho V_0}{\omega} + \ln(F/K)\ . \tag{40}$$

The initial values $f_j(0)$ are given in propositions 3.2 and 3.3.

The proof can be found in appendix A.

Equation (38) shows that the asymptotic decay of the integrand is at least exponential. In particular, $C_\infty > 0$ guarantees the existence of the integral. A simple and reliable transformation is to translate the integration according to

$$\int_0^\infty f_j(u)\,\mathrm{d}u \;=\; \int_0^1 \frac{f_j(u(x))}{x \cdot C_\infty}\,\mathrm{d}x \tag{41}$$

with

$$u(x) \;=\; -\frac{\ln x}{C_\infty}\,. \tag{42}$$

The transformation is only possible when $C_\infty > 0$. Fortunately, this is given as long as $|\rho| \neq 1$.

One last step is needed before we can proceed with the implementation. Looking at the functions f_j in (4), we can see that $f_j(u)$ is, strictly speaking, not defined at $u = 0$. The continuity of the function at zero in figures 1 and 2 gives us hope, though, that we can find the value analytically by the aid of l'Hospital's rule.

Proposition 3.2 The function

$$f_1(u) = \mathrm{Re}\left(\frac{\mathrm{e}^{-iu\ln K}\varphi(u-i)}{iuF}\right) \tag{43}$$

has the following property at zero:

$$\lim_{u\to 0} f_1(u) = \ln(F/K) + \mathrm{Im}\left(C'(-i)\right) + \mathrm{Im}\left(D'(-i)\right)\cdot V_0 \tag{44}$$

with

$$\mathrm{Im}\left(C'(-i)\right) \;=\; \frac{\mathrm{e}^{(\rho\omega-\kappa)\tau}\theta\kappa + \theta\kappa((\kappa-\rho\omega)\tau - 1)}{2(\kappa-\rho\omega)^2} \tag{45}$$

$$\mathrm{Im}\left(D'(-i)\right) \;=\; \frac{1-\mathrm{e}^{-(\kappa-\rho\omega)\tau}}{2(\kappa-\rho\omega)}, \tag{46}$$

provided that $(\kappa - \rho\omega) \neq 0$. When $(\kappa - \rho\omega) = 0$, we obtain

$$\mathrm{Im}\left(C'(-i)\right) \;=\; \frac{\kappa\theta\tau^2}{4} \tag{47}$$

$$\mathrm{Im}\left(D'(-i)\right) \;=\; \frac{\tau}{2}\,. \tag{48}$$

The proof can be found in Appendix A.

Proposition 3.3 The function

$$f_2(u) = \mathrm{Re}\left(\frac{\mathrm{e}^{-iu\ln K}\varphi(u)}{iu}\right) \tag{49}$$

has the following property at zero:

$$\lim_{u\to 0} f_2(u) = \ln(F/K) + \mathrm{Im}\left(C'(0)\right) + \mathrm{Im}\left(D'(0)\right)\cdot V_0 \tag{50}$$

with

$$\mathrm{Im}\left(C'(0)\right) \;=\; -\frac{\mathrm{e}^{-\kappa\tau}\theta\kappa + \theta\kappa(\kappa\tau - 1)}{2\kappa^2} \tag{51}$$

$$\mathrm{Im}\left(D'(0)\right) \;=\; -\frac{1-\mathrm{e}^{-\frac{1}{2}\kappa\tau}}{2\kappa}\,. \tag{52}$$

The proof can also be found in Appendix A.

The above analysis enables us to implement the required Fourier inversion as a Gauss-Lobatto integration over the interval $[0, 1]$ using the transformation given by (41), (42), and (39). Since Gauss-Lobatto quadrature evaluates its integrand at the boundary values, we need to use the analytical limit values (44) and (50) for the evaluation of $f_j\left(u(x)\right)|_{x=1}$. The limit values at $x = 0$ seem at first sight to be more complicated. However, it is straightforward to see from equation (38) that those limit values are zero as long as $C_\infty > 0$ which in turn is given as long as $|\rho| < 1$.

In practice, we combine all calculations in (3) into the single numerical integration for the undiscounted call option price

$$C(S, K, V_0, \tau)/P(\tau) \;=\; \int_0^1 y(x)\,\mathrm{d}x \tag{53}$$

with

$$y(x) \;:=\; \frac{1}{2}(F - K) + \frac{F \cdot f_1(-\frac{\ln x}{C_\infty}) - K \cdot f_2(-\frac{\ln x}{C_\infty})}{x \cdot \pi \cdot C_\infty} \tag{54}$$

and $F = S \cdot \mathrm{e}^{\mu\tau}$, as before. The limits of $y(x)$ at the boundaries of the integral are

$$\lim_{x\to 0} y(x) \;=\; \frac{1}{2}(F - K) \tag{55}$$

and

$$\lim_{x\to 1} y(x) \;=\; \frac{1}{2}(F - K) + \frac{F \cdot \lim_{u\to 0} f_1(u) - K \cdot \lim_{u\to 0} f_2(u)}{\pi \cdot C_\infty} \tag{56}$$

with $\lim_{u\to 0} f_1(u)$ and $\lim_{u\to 0} f_2(u)$ given by (44) and (50), respectively. An example for the set of sampling points chosen by the adaptive Gauss-Lobatto scheme for a target accuracy of 10^{-6} is shown in figure 6.

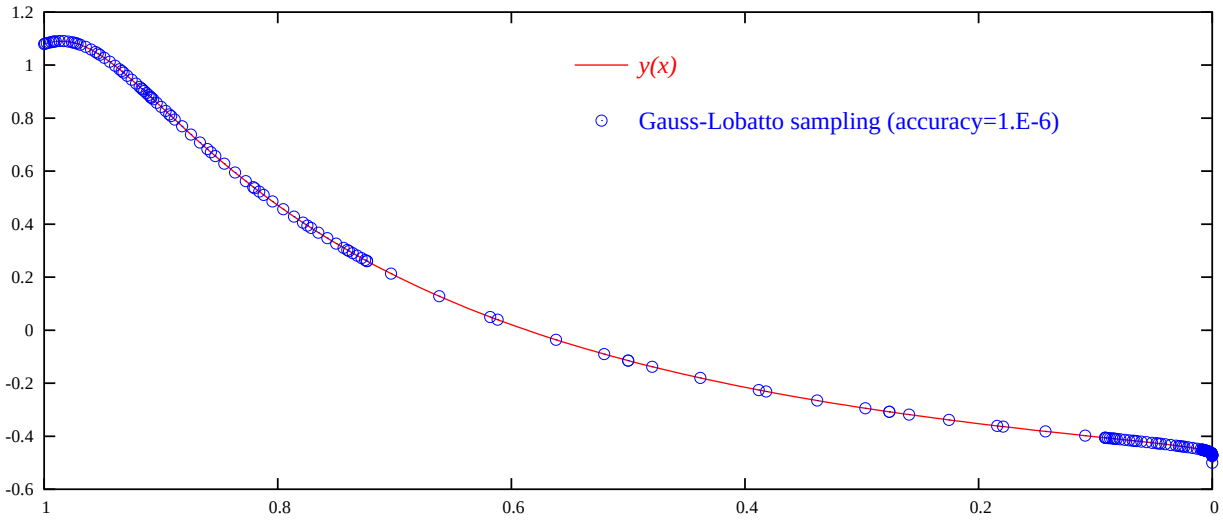

Figure 6: The sampling points selected by the adaptive Gauss-Lobatto scheme for the integration of equation (53). $S = F = 1$, $\mu = 0$, $V_0 = \theta = 0.16$, $\kappa = 1$, $\omega = 2$, $\rho = -0.8$, $\tau = 10$, $K = 2$. The total number of evaluation points was 198, and the resulting integral value was 4.95212%.

The stability of Gauss-Lobatto integration over the interval $x \in [0, 1]$ of the transformed integrand $f_j(u(x))/\left(x \cdot C_\infty\right)$ as described is such that even extremely far out-of-the-money option prices can be computed, as well as very long dated maturities. We demonstrate this in figure 7, where implied Black volatilities are displayed for the same parameters as previously used in figure 4.

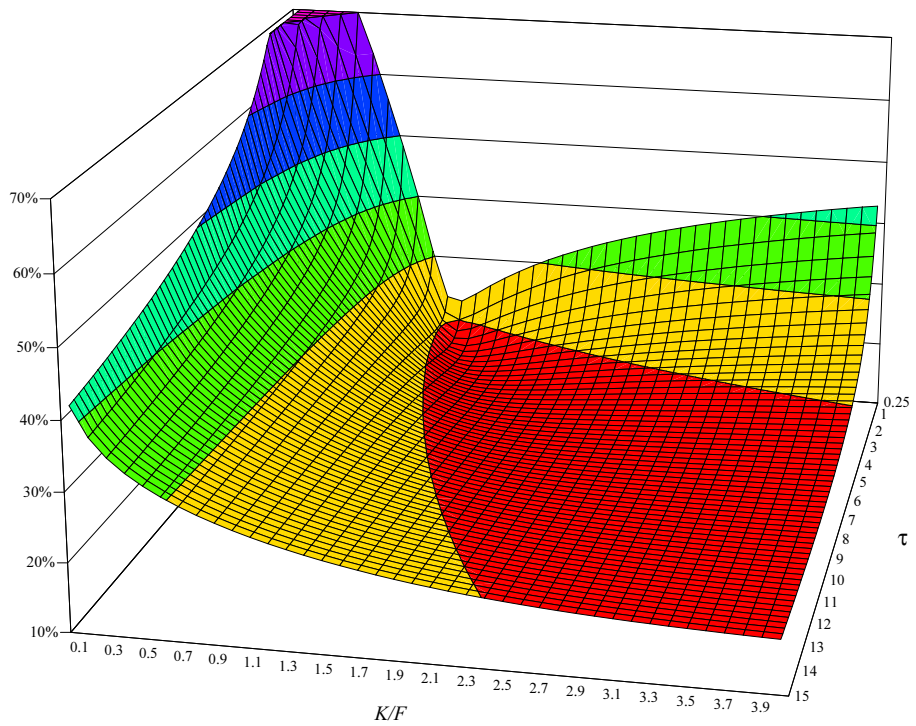

Figure 7: Black implied volatilities from the Heston model. Underlying: $\mathrm{d}S_t = \mu S_t \mathrm{d}t + \sqrt{V_t} S_t \mathrm{d}W_S(t)$ with $S = F = 1$ and $\mu = 0$. Variance: $\mathrm{d}V_t = \kappa(\theta - V_t)\mathrm{d}t + \omega\sqrt{V_t}\mathrm{d}W_V(t)$ with $V_0 = \theta = 0.16$, $\kappa = 1$, $\omega = 2$, $\rho = -0.8$, $\tau \in [1/4, 15]$, and $K \in [1/10, 4]$.

4 Conclusion

The problem we addressed was that Fourier inversion integrals of the form (3) used for the calculation of option prices based on analytical knowledge of the log-characteristic function of the underlying stochastic process are particularly prone to numerical instabilities due to their involved complex logarithms and complex power expressions. We found that the difficulty is ultimately not, as was previously reported, caused by the multivalued nature of the *complex logarithm*, but instead by the multivalued nature of the *complex power function*. We analysed this issue for the Heston stochastic volatility model, though, the key insight is readily transferable to the calculation of option prices in other models that are amenable to the Fourier inversion integral approach [Car03, CM99] based on a log-characteristic function. We also presented a detailed analysis how the Fourier integral itself can be computed reliably by the aid of adaptive Gauss-Lobatto quadrature, using asymptotic analytical methods to identify the most suitable transformation from the half-open integration domain $[0, \infty)$ to the interval $[0, 1]$. These results, too, are not only useful for the purpose of computing option prices for the Heston model, but also to illustrate how similar methods can be devised for other models that are to be evaluated with Fourier integration techniques.

A Proofs

In this section we present the missing proofs of sections 2 and 3.

Proof:[Prop. 2.1] First we need some preliminary calculation

$$c(u) = \frac{\kappa - \rho\omega u i + d(u)}{\kappa - \rho\omega u i - d(u)} \tag{57}$$

$$= \frac{\kappa - \rho\omega u i + (a_d + i b_d)}{\kappa - \rho\omega u i - (a_d + i b_d)} \tag{58}$$

$$= \frac{(\kappa + a_d) + i\,(-\rho\omega u + b_d)}{(\kappa - a_d) - i\,(\rho\omega u + b_d)} \tag{59}$$

$$= \frac{[(\kappa + a_d) + i\,(-\rho\omega u + b_d)]\,[(\kappa - a_d) + i\,(\rho\omega u + b_d)]}{[(\kappa - a_d) - i\,(\rho\omega u + b_d)]\,[(\kappa - a_d) + i\,(\rho\omega u + b_d)]} \tag{60}$$

$$= \frac{\kappa^2 + (\rho\omega u)^2 - \left(a_d^2 + b_d^2\right) + i\,(b_d \cdot \kappa + a_d \cdot \rho\omega u)}{C} \tag{61}$$

Hence we have to show if

$$b_d \cdot \kappa = -a_d \cdot \rho\omega u\ , \tag{62}$$

that

$$\kappa^2 + (\rho\omega u)^2 - \left(a_d^2 + b_d^2\right) < 0\ . \tag{63}$$

First we can deduce from (62) that

$$\rho\omega u = \frac{-b_d \kappa}{a_d}\ . \tag{64}$$

Using this in the left hand side of (63) we obtain

$$\kappa^2 + (\rho\omega u)^2 - \left(a_d^2 + b_d^2\right) = \frac{a_d^2 + b_d^2}{a_d^2}\left(\kappa^2 - a_d^2\right) < 0\ . \tag{65}$$

Let

$$d(u) = \sqrt{i \cdot \underbrace{u\left(\omega^2 - 2\kappa\rho\omega\right)}_{q(u)} + \underbrace{\omega^2 u^2\left(1 - \rho^2\right) + \kappa^2}_{p(u)}}\,, \tag{66}$$

$$z(u) = i \cdot q(u) + p(u) = r(u)\,(\cos(\varphi) + i\sin(\varphi))\ . \tag{67}$$

Thus

$$a_d^2(u) = r(u)\cos^2(\tfrac{\varphi}{2}) \tag{68}$$

$$> r(u)\cos(\varphi) \tag{69}$$

$$= \omega^2 u^2\left(1 - \rho^2\right) + \kappa^2 \tag{70}$$

$$\geq \kappa^2 \tag{71}$$

which completes the proof. □

Proof:[Prop. 3.1] The proof of equation (34) is basic analysis:

$$\lim_{u\to\infty}\frac{d(u)}{u} = \lim_{u\to\infty}\sqrt{\omega^2(1-\rho^2) - 2i\omega(\rho\kappa - \frac{1}{2}\omega)\Big/ u + \kappa^2/\,u^2} \tag{72}$$

$$= \omega\sqrt{1-\rho^2}$$

Using this result, we are able to confirm equation (35)

$$\begin{aligned}\lim_{u\to\infty} c(u) &= \frac{-\rho\omega i+\omega\sqrt{1-\rho^2}}{-\rho\omega i-\omega\sqrt{1-\rho^2}}\\ &= -\frac{(\omega\sqrt{1-\rho^2}-\rho\omega i)^2}{\omega^2(1-\rho^2)+\rho^2\omega^2}\\ &= -\frac{\omega^2(1-\rho^2)-2i\omega^2\rho\sqrt{1-\rho^2}-\rho^2\omega^2}{\omega^2}\\ &= -1+2\rho^2+2i\rho\sqrt{1-\rho^2}=\left(i\sqrt{1-\rho^2}+\rho\right)^2 . \qquad (73)\end{aligned}$$

Note that $\lim_{u\to\infty}|c(u)|=1$. In order to show equation (36), we need the calculation

$$\begin{aligned}\lim_{u\to\infty}\left[\frac{\mathrm{e}^{d(u)\tau}-1}{c(u)\mathrm{e}^{d(u)\tau}-1}\right] &= \lim_{u\to\infty}\left[\frac{1}{c(u)}\left(1+\frac{1-c(u)}{c(u)\mathrm{e}^{d(u)\tau}-1}\right)\right]\\ &= \lim_{u\to\infty}\frac{1}{c(u)}\\ &= \lim_{u\to\infty}\frac{\overline{c(u)}}{|c(u)|} \qquad (74)\\ &= -1+2\rho^2-2i\rho\sqrt{1-\rho^2}\,. \qquad (75)\end{aligned}$$

$$\begin{aligned}\lim_{u\to\infty}\frac{D(u)}{u} &= \frac{1}{\omega^2}\cdot(-1+2\rho^2-2i\rho\sqrt{1-\rho^2})(-\rho\omega i+\omega\sqrt{1-\rho^2})\\ &= \frac{-i\rho-\sqrt{1-\rho^2}}{\omega}. \qquad (76)\end{aligned}$$

Finally, we prove (37)

$$\begin{aligned}\lim_{u\to\infty}\ln\left[\frac{c(u)\mathrm{e}^{d(u)\tau}-1}{c(u)-1}\right]/u &= \lim_{u\to\infty}\ln\left[\mathrm{e}^{d(u)\tau}\frac{c(u)}{c(u)-1}\right]/u \qquad (77)\\ &= \lim_{u\to\infty}\left(\ln\left[\mathrm{e}^{d(u)\tau}\right]+\ln\left[\frac{c(u)}{c(u)-1}\right]\right)/u \qquad (78)\\ &= \lim_{u\to\infty} d(u)\tau/u = d_\infty\tau. \qquad (79)\end{aligned}$$

From here, we obtain

$$\lim_{u\to\infty}\frac{C(u)}{u} = -\alpha\tau\left(d_\infty+i\omega\rho\right). \qquad (80)$$

Combination of the limit results for $D(u)$ and $C(u)$ makes it straightforward to arrive at the statements (38) and (39) for $f_j(u)$. □

Proof:[Prop. 3.2] Considering the function f_1 as given in (4) we see that

$$\lim_{u\to 0} f_1(u) = \lim_{u\to 0}\mathrm{Im}\left[\mathrm{e}^{iu\ln(F/K)}\frac{\mathrm{e}^{C(\tau,u-i)+D(\tau,u-i)\cdot V_0+\ln(F)}}{uF}\right]. \qquad (81)$$

The expressions that need attention for the evaluation of this limit are $\lim_{u\to 0} C(\tau,u-i)$ as well as $\lim_{u\to 0} D(\tau,u-i)$. We start with

$$\lim_{u\to 0} d(u-i) = |\kappa-\rho\omega|\,. \qquad (82)$$

The limit $\lim_{u\to 0} c(u-i)$ depends on the sign of $\kappa - \rho\omega$. We first consider the case where $\kappa - \rho\omega < 0$. We obtain

$$\lim_{u\to 0} c(u-i) = \lim_{u\to 0} \frac{\kappa - i\rho\omega(u-i) + d(u-i)}{\kappa - i\rho\omega(u-i) - d(u-i)} = 0\ . \tag{83}$$

This allows us to deduce

$$\lim_{u\to 0} D(u-i) = 0, \qquad \lim_{u\to 0} C(u-i) = 0. \tag{84}$$

The case $\kappa - \rho\omega > 0$ is a little bit more complicated. First we see that

$$\lim_{u\to 0} |c(u-i)| = \lim_{u\to 0} \frac{|\kappa - i\rho\omega(u-i) + d(u-i)|}{|\kappa - i\rho\omega(u-i) - d(u-i)|} = \infty \tag{85}$$

as the denominator goes to zero. Using this we can see that

$$\lim_{u\to 0} D(u-i) = \lim_{u\to 0} \frac{\kappa - i\rho\omega(u-i) + d(u-i)}{\omega^2} \left(\frac{\mathrm{e}^{d(u-i)\tau} - 1}{c(u-i)\mathrm{e}^{d(u-i)\tau} - 1} \right) \tag{86}$$

$$= 0\ . \tag{87}$$

Furthermore, we have

$$\lim_{u\to 0} C(u-i) = \lim_{u\to 0} \alpha \left((\kappa - i\rho\omega(u-i) + d(u-i))\tau - 2\ln\left[\mathrm{e}^{d(u-i)\tau} + \frac{\mathrm{e}^{d(u-i)\tau} - 1}{c(u-i) - 1} \right] \right) \tag{88}$$

$$= 0\ . \tag{89}$$

Last we have to check the case $\kappa - \rho\omega = 0$. First we have to notice that

$$\lim_{u\to 0} \frac{d(u-i)}{\sqrt{u}} = \lim_{u\to 0} \sqrt{\omega^2(1-\rho^2)u - i\omega^2} = \sqrt{-i\omega^2}. \tag{90}$$

We have to mention that this limit is not zero as $\omega \neq 0$ if $\kappa - \rho\omega = 0$ and $\kappa > 0$. Using this we obtain

$$\lim_{u\to 0} c(u-i) = -1 + \lim_{u\to 0} \frac{-2\rho\omega u i}{-\rho\omega u i - d(u-i)} \tag{91}$$

$$= -1 + \lim_{u\to 0} \frac{2\rho\omega i\sqrt{u}}{\rho\omega i\sqrt{u} + \sqrt{-i\omega^2}} = -1\ . \tag{92}$$

Again we get $\lim_{u\to 0} D(u-i) = 0$ and

$$\lim_{u\to 0} C(u-i) = \alpha \cdot \lim_{u\to 0} \left((\kappa - \rho\omega + d(u-i))\tau - 2\ln\left[\frac{c(u-i)\mathrm{e}^{d(u-i)\tau} - 1}{c(u-i) - 1} \right] \right) \tag{93}$$

$$= \alpha \cdot \ln\left[\frac{2}{2}\right] = 0\ . \tag{94}$$

Hence in all different cases

$$\lim_{u\to 0} \mathrm{e}^{iu\ln(F/K) + C(u-i) + D(u-i)V_0} = 1\ . \tag{95}$$

Now we decompose the exponent into a real and imaginary part

$$iu\ln(F/K) + C(\tau, u-i) + D(\tau, u-i)\cdot V_0 =: H(u) + iJ(u) \tag{96}$$

with functions $H, J : \mathbb{R} \longrightarrow \mathbb{R}$. Due to (95), we also know that

$$\lim_{u\to 0} H(u) = 0\ , \qquad \lim_{u\to 0} J(u) = 0\ . \tag{97}$$

Now we can calculate

$$f_1(0) = \lim_{u\to 0} \mathrm{Im}\left[\frac{\mathrm{e}^{H(u)+iJ(u)}}{u}\right] \tag{98}$$

$$= \lim_{u\to 0} \mathrm{Im}\left[\mathrm{e}^{H(u)}\frac{\cos(J(u))+i\sin(J(u))}{u}\right] \tag{99}$$

$$= \lim_{u\to 0} \mathrm{e}^{H(u)}\frac{\sin(J(u))}{u} \tag{100}$$

$$= \lim_{u\to 0} \mathrm{e}^{H(u)} \cdot \lim_{u\to 0} \frac{\sin(J(u))}{u} \tag{101}$$

$$= \lim_{u\to 0} J'(u)\frac{\cos(J(u))}{1} = \lim_{u\to 0} J'(u)\ , \tag{102}$$

where we applied the rule of l'Hospital in the last step. Thus,

$$f_1(0) = \lim_{u\to 0} J'(u) = J'(0) = \ln(F/K) + \mathrm{Im}\left(C'(-i)\right) + \mathrm{Im}\left(D'(-i)\right)V_0\ . \tag{103}$$

The computation of C' and D' is tedious but straightforward. We obtain

$$\mathrm{Im}\left(C'(-i)\right) = \frac{\mathrm{e}^{(\rho\omega-\kappa)\tau}\theta\kappa + \theta\kappa((\kappa-\rho\omega)\tau - 1)}{2(\kappa-\rho\omega)^2}, \tag{104}$$

$$\mathrm{Im}\left(D'(-i)\right) = \frac{1-\mathrm{e}^{-(\kappa-\rho\omega)\tau}}{2(\kappa-\rho\omega)}, \tag{105}$$

if $(\kappa - \rho\omega) \neq 0$, and otherwise

$$\mathrm{Im}\left(C'(-i)\right) = \frac{\kappa\theta\tau^2}{4}, \tag{106}$$

$$\mathrm{Im}\left(D'(-i)\right) = \frac{\tau}{2}, \tag{107}$$

which completes the proof. □

Proof:[Prop. 3.3] The proof of the limit $\lim_{u\to 0} f_2(u)$ can be done in complete analogy to the proof of $\lim_{u\to 0} f_1(u)$. □

References

[Car03] P. Carr. Option Pricing using Integral Transforms, 2003. www.math.nyu.edu/research/carrp/papers/pdf/integtransform.pdf.

[CM99] P. Carr and D.B. Madan. Option valuation using the fast Fourier transform. *Journal of Computational Finance*, 2(4):61–73, 1999.

[GG00] W. Gander and W. Gautschi. Adaptive Quadrature — Revisited. *BIT*, 40(1):84–101, March 2000. CS technical report: ftp.inf.ethz.ch/pub/publications/tech-reports/3xx/306.ps.gz.

[Hes93] S. L. Heston. A closed-form solution for options with stochastic volatility with applications to bond and currency options. *The Review of Financial Studies*, 6:327–343, 1993.

[Lee05] R. Lee. Option Pricing by Transform Methods: Extensions, Unification, and Error Control. *Journal of Computational Finance*, 7(3):51–86, 2005.

[MN03] S. Mikhailov and U. Nögel. Heston's Stochastic Volatilty Model: Implementation, Calibration, and some Extensions. *Wilmott*, July:74–79, 2003.

[Sep04] A. Sepp. Pricing European-Style Options under Jump Diffusion Processes with Stochastic Volatility: Applications of Fourier Transform. *Acta et Commentationes Universitatis Tartuensis de Mathematica*, 8:123–133, 2004. math.ut.ee/~spartak/papers/stochjumpvols.pdf.

[SZ99] R. Schöbel and J. Zhu. Stochastic Volatility With an Ornstein Uhlenbeck Process: An Extension. *European Finance Review*, 3:23–46, 1999. pluto.huji.ac.il/~efr/3/3_1schoebel.pdf.